Adsorption of imidazolium and pyridinium ionic liquids onto montmorillonite: characterization and thermodynamic calculations

L. Reinert, Khaled Batouche, Jean-Marc Lévêque, Fabrice Muller, Jean-Michel Bény, Brahim Kebabi, L. Duclaux

Adsorption of imidazolium and pyridinium ionic liquids onto montmorillonite : characterization and thermodynamic calculations

Laurence Reinert[a*], Khaled Batouche[b], Jean-Marc Lévêque[a], Fabrice Muller[c], Jean-Michel Bény[c], Brahim Kebabi[b], Laurent Duclaux[a]

[a]LCME, Université de Savoie, Savoie Technolac, 73376 Le Bourget du Lac Cedex, France
[b]LPTE, Université Mentouri, Constantine 25000, Algérie
[c]ISTO, CNRS-Université d'Orléans, 45071 Orléans Cedex 2, France

* corresponding author : Laurence Reinert
e-mail address : laurence.reinert@univ-savoie.fr
Tel : 33 (0)4 79 75 81 22
Fax : 33 (0)4 79 75 86 74

Abstract

Five first generation ionic liquids (RTILs : BMImCl, OMImCl, AMImCl, BPyBr and OPyBr) were intercalated into the layered structure of a Na-montmorillonite by dispersion in aqueous solutions ([RTIL] ≤ 20 mmol.L^{-1}). For all ionic liquids, the intercalation expanded the spacing of the silicate layers, as measured by X-ray diffraction. FTIR, thermogravimetric analyses and sodium titrations of the solutions after intercalation proved the adsorption of the RTILs through a cation exchange mechanism. Adsorption isotherms, done at pH = 7 and at 25°C, displayed that the maximum adsorption capacity of the substrates was closely linked to the nature of the organic cation and the length of the alkyl chain (BPyBr > OPyBr ~ AMImCl ~ BMImCl > OMImCl). For the five RTILs, calculated parameters obtained from the adsorption isotherms studied at 3 temperatures (25°C, 40°C and 55°C) concluded to an endothermic and spontaneous adsorption reaction.

Keywords: Montmorillonite; Ionic liquids; Adsorption; Thermodynamic parameters

1. Introduction

Room Temperature Ionic liquids (RTILs) are organic salts with low melting points (< 100°C) and thermally stable [1]. Due to their extremely low vapour pressures [2], they constitute an attractive alternative to traditional solvents and are thus widely used as green solvents for various applications [1,3,4]. RTILs are formed by the combination of nitrogen, phosphorus or sulphur containing organic cations (for example alkylimidazolium, alkylpyridinium,

alkylphosphonium or alkylammonium…) with organic or inorganic anions (BF_4^-, PF_6^-, CF_3COO^-, Cl^-, Br^-…).

It is well known that many ionic liquids are soluble in water. A foreseen industrial use may thus be a source of pollution as they can be released in the environment via industrial liquid effluents. Many recent researches highlighted that the toxicity and ecotoxicity of ionic liquids may have an impact on the environment [5]. It is thus needed to find solutions for their removal.

Like other organic wastes, RTILs can be adsorbed through different mechanisms by various adsorbents, as example activated carbons [6], layered zirconium phosphates [7] and nano-silica [8]. The adsorption capacity of natural soils [9] and sediments [10,11] is limited and strongly dependent on their composition.

Since recently, several researches reported the intercalation of various ionic liquids into the interlamellar spaces of clays. Kaolinite was used for the adsorption of an ethyl-pyridinium chloride [12] and pyrrolidinium halides [13]. However, as the direct intercalation was unsuccessful, urea and DMSO pre-intercalated kaolinites had to be prepared before the RTILs intercalation. Smectites were modified by adsorption of mono-cationic and di-cationic ionic liquids [14] in order to produce suitable matrices for the adsorption of the tetracycline pollutant drug. Sodium montmorillonites were used for the intercalation of many RTILs, as example imidazolium [15,16,17], pyridinium [18] or phosphonium salts [19]. The aim of these studies was to produce fillers for the elaboration of nanocomposites, as ionic liquids possess interesting thermal properties. Montmorillonite was also used for the adsorption of 1-n-alkylpyridinium bromides [20], adsorption isotherms were studied at room temperature to determine the influence of the length of the alkyl chain on the adsorption capacity of the clay. RTIL-intercalated clays can thus be used in various field, very recent researches specify the use of these organo-clays as supports for catalytic syntheses [18].

The aim of this present work is to study the adsorption capacity of a Na-montmorillonite towards various first generation ionic liquids which are water soluble and dissociated, enabling a cationic exchange between the clay and the chosen organic cations. The cation exchange capacity of montmorillonite typically ranges between 80-150 meq/100g [21] making this material a suitable adsorbent for ionic liquids, through a cation exchange mechanism. Imidazolium chlorides and pyridinium bromides with butyl, octyl, or allyl chains were chosen to study the effect of the nature of cation and alkyl chain on adsorption. Adsorption isotherms were studied at three different temperatures to determine the thermodynamic parameters of adsorption.

2. Experimental

The five ionic liquids (Table 1) were synthesized in our laboratory according to already published procedures. 1-methyl-3-butylimidazolium chloride (BMImCl) and 1-methyl-3-octylimidazolium chloride (OMImCl) were synthesised through a neat procedure under microwave irradiation [22]. 1-allyl-3-methylimidazolium chloride (AMImCl) was also synthesised through a neat procedure under mechanical stirring [23]. Briefly, 1-methylimidazole and allyl chloride (molar ratio 1:1.25) were mixed in a round-bottomed flask fitted with a reflux condenser for 8 h at 55 °C with stirring. After appropriate time, the resulting solution was dried under high vacuum for 12 h to remove unreacted reagents and water traces to afford a slightly amber liquid. 1-butylpyridinium bromide (BPyBr) [24] and 1-octylpyridinium bromide (OPyBr) [25] were also synthesised according to known procedures. To better complete the purification, all synthesised ionic liquids were successively washed with diethylether, cyclohexane and ethyl-acetate [26] and then dried under vacuum for several days (typically 2 days) using a primary vacuum (10^{-3} mbar) pump equipped with a liquid nitrogen trap in order to remove the remaining traces of solvent or unreacted reagents.
The molecules geometry was defined using Chemsketch 3D. The molecule dimensions were calculated from a parallelepiped box containing the molecule. Typically, the height direction was chosen along the direction perpendicular to the aromatic plane of the cation, the length direction was chosen along a direction close to the chain length and parallel to the aromatic plane, and the width direction was parallel to the aromatic plane and perpendicular to the length direction.

The mother RTILs solutions (30 mmol.L^{-1}) were prepared by dissolving a weighted amount of dried ionic liquid in Ultra High Quality water (18.2 MΩ purity).
A Kunipia Na-montmorillonite (MMT) from Kunimine Industries (Japan) obtained by purification of a bentonite was used as adsorbent. The cation exchange capacity of this MMT was equal to 115 meq/100g. Before adsorption experiments, MMT was washed in distilled water under stirring for 12 h. Five consecutive washings were necessary to reach a constant pH, the MMT powder was then recovered by centrifugation (3000 rpm) and dried at 230°C for 24 h.
Adsorption was achieved by agitation of a dispersion of MMT (typically 0.05 g of clay) in 25 mL of various aqueous ionic liquid solutions ([RTIL] = 0.5 to 7 mmol.L^{-1} for adsorption isotherms and 30 mmol.L^{-1} for TGA experiments) at 25°C, 40°C or 55°C, at pH = 7, for 30 min. Indeed, the kinetics of adsorption of the five ionic liquids (results not presented) were found very quick (15 min). The intercalated MMT was recovered by filtration under vacuum and washed with distilled water until no trace of chloride or bromide were detected in the filtrate (by titration with a 0.1 mol.L^{-1} $AgNO_3$ solution).
Desorption experiments were performed by agitation of 0.2 g of intercalated clay dispersed in 25 mL of deionised water for 24 h.

After adsorption or desorption, the remaining RTILs concentrations in the aqueous solutions were determined by UV-Visible spectrometry (Varian, Cary50). The maximum absorbances were obtained at 211 nm for AMImCl, BMImCl and OMImCl and 259 nm for OPyBr and BPyBr.

Sodium concentrations in solution were determined using a JENWAY PFP7 emission flame photometer (working fuel : propane, limit of detection : Na ≤ 0.2 ppm).

Thermogravimetric analyses were performed in a homemade apparatus equipped with a Mettler balance (± 0.1 mg). About 200mg of sample were heated from 25 to 1000°C with a heating rate of 4°C.min^{-1} under air.

The crystalline structure of the samples was characterized by X-ray diffraction (XRD) using a Thermo Electron ARL'XTRA diffractometer in Bragg-Brentano (θ, θ) mode goniometer. The device was equipped with a Si(Li) solid detector filtering the $Cu_{K\alpha}$ radiation ($\lambda Cu_{K\alpha}$ = 1.5418 Å) of a standard European type X-ray tube (40 kV, 40 mA). The divergence, the incident beam scatter, the diffracted beam scatter and the receiving slits were 2.00, 4.00, 0.50 and 0.22 mm wide, respectively. XRD patterns were collected from 2° to 24° 2θ at a scan rate of 0.3° 2θ/min by step of 0.05° 2θ.

Fourier Transform Infrared (FTIR) spectra were recorded using a Nicolet Magma-IR 760 Fourier Transform spectrometer. It was purged with dry air to remove most of the atmospheric H_2O and CO_2. The resolution was 2 cm^{-1} and the number of scans was 128 to give spectra with good Signal/Noise ratios; the studied wave number range was 400-4000 cm^{-1} according to the spectrometer beam splitter and detector (Deuterium Triglycine Sulphate). The analyses were performed in transmission mode. About 0.5 mg clay were finely grounded and mixed with KBr. This mixture (150 mg) was pressed under 370 MPa pressure in a die to produce a pellet.

3. Results and discussion

3.1 Adsorption studies

3.1.1 X-ray diffraction analyses

The X-ray diffraction pattern of raw MMT exhibits a *00l* peak centred at 2θ = 7.30° (Figure 1a) corresponding to a basal d-spacing of 12.13 Å (Table 2). For the ionic liquid modified montmorillonites, the *00l* characteristic peak of the clay was shifted to lower 2θ values (Figure 1), leading to an increase of the interlayer spacing (Table 2). This shift is a clear signature of the intercalation of the RTILs between the layers of MMT. For the intercalated imidazolium or pyridinium moieties, the interlayer distances are clearly influenced by the length of the alkyl substituent grafted on the different ionic liquids. Indeed, the d-spacing

increased as the alkyl group length and thus the average steric size [27] of the cation increased (Tables 1 and 2). The highest interlayer distances were observed for the octyl chains as expansions of 1.67 Å and 1.78 Å were measured after OMImCl and OPyBr intercalation, respectively (Table 2). For the intercalation of the ionic liquid with the shortest alkyl group (i.e. the allyl group), an expansion of only 0.67 Å was observed. The nature of the organic cation had no clear influence on the expansion of the clay, as for similar alkyl groups the difference in d-spacing was only of ~ 0.1 Å for both imidazolium and pyridinium cations. These results suggest that the swelling of the clay is directly related to the steric size of the intercalated molecule and are in good agreement with previous studies [15, 18].
The large *00l* peak of MMT became sharper and more symmetrical after intercalation of the different ionic liquids. The narrow shape of the peaks suggests that the RTILs induced a better ordering in the stacking of the sheets (Figure 1). The increase in d-spacing after intercalation was low and ranged between ~ 0.7 Å (in the case of AMImCl) and ~ 1.8 Å (in the case of OPyBr). The d-spacing expansion values were below or very close to the simulated heights of the ionic liquid cations (Table 1, ~ 1.8 Å), suggesting that the pyridinium and imidazolium cations were probably lying flat between the mineral sheets and arranged as a monolayer, parallel to the sheets.

3.1.2 Thermogravimetric determination of the RTIL intercalated amount

TGA curves of pure ionic liquids show that the decomposition of the organics started at ~ 200°C and was complete in the range 300°C-500°C, depending on the ionic liquid type (Figure 2). Pyridinium salts usually possess a lower thermal stability than imidazolium ones [28, 29]. The TGA analyses confirmed this general trend as OPyBr and BPyBr started and finished decomposing before the three imidazolium molecules (Figure 2a and b). Whatever the cation type, the thermal stability of the octyl ionic liquid was lower than the butyl one. This is in agreement with the general trends observed for different IL families: the stability of the RTILs decreases as the alkyl group attached to nitrogen increases [31]. The fact that AMImCl starts decomposing before OMImCl and BMImCl can be explained by the higher reactivity of the double bond of the allyl group compared to saturated alkyl chains [30]. According to the literature, the halide (Br^- or Cl^-) should not have any significant influence on the decomposition temperature of the pure ionic liquids [31]. The thermal stability of the five pure RTILs thus followed the trend OPyBr < BPyBr < AMImCl < OMImCl < BMImCl (Figure 2).
The TGA curve of raw MMT depicts a first weight loss from room temperature up to about 100°C (Figure 3 : ~ 9%) that was attributed to the elimination of adsorbed water. In this temperature range, a small weight loss of maximum 1 % was observed for RTILs-intercalated montmorillonites, indicating that the ionic liquids intercalation afforded hydrophobic

montmorillonites. The weight loss of ~ 4.5% observed between ~ 570°C and 800°C on the raw MMT curve was attributed to the dehydroxylation of structural hydroxyl groups [32]. The thermal decomposition of the various intercalated RTILs began at similar temperatures than those determined for pure ionic liquids (Figure 3 : ~ 250 °C) but continued then much more slowly. In addition, the weight loss observed in the range 500-1000°C could not be exclusively attributed to the dehydroxylation phenomenon of the clay as it was greater for the intercalated montmorillonites (~ 8 to 13 %) than for the pure one (~ 4.3 %). This suggested that the organic matter decomposition was superimposed to the dehydroxylation of MMT. Derivative TGA curves (DTG) of intercalated montmorillonites confirmed that the dehydroxylation started before the complete ionic liquids decomposition, as DTG peaks are superimposed around 570°C (Figure 4), which is the starting temperature for dehydroxylation of pure MMT (Figure 3). The extended temperature domain for the decomposition of the intercalated RTILs could have different origins. It might be explained either by the barrier properties of the clay mineral layers which hindered the oxygen molecules diffusion needed to decompose the organic matters or by the absence of the halides (Cl^- and Br^- were fully removed from the samples by washing after the cationic exchange) known to catalyse the decomposition process [33].

DTG curves of both pyridinium ILs and of OMImCl present two distinct maxima in the range 200°C – 570°C whereas shoulders are observed at ~300°C on the peaks attributed to the IL decomposition of AMImCl and BMImCl intercalated MMTs (Figure 4). This two steps decomposition suggests the presence of few amounts of ILs physisorbed on the clay surface (leading to the lowest temperatures peaks, identified at the same temperature than the temperature of decomposition of pure ionic liquids) and of mainly chemisorbed (exchanged) ILs (responsible for the intense second peaks below ~570°C).

By assuming that all organic intercalated montmorillonites display a similar dehydroxylation rate (i.e. ~ 4.3 mass. % of the clay content), the molar intercalated ionic liquid cation content could be approximately calculated from the total mass losses (Figure 3). From these calculations, a first trend emerged for the IL cation molar content giving the order $BPy^+ > OPy^+ \sim AMIm^+ \sim BMIm^+ > OMIm^+$.

At 25°C, the desorption measured for OPy^+, BPy^+ and $OMIm^+$ (in aqueous solution, see experimental part) was of about 2 mass. % whereas it was lower than 1 mass. % for $AMIm^+$ and $BMIm^+$. The amount of ionic liquid desorbed is in accordance with the low amount of physisorbed cations determined by TGA (Figure 3) and DTG analyses (Figure 4, first peak or shoulder observed on DTG peaks between about 200 and 330°C).

The effect of the ionic strength on the adsorption of BMImCl was studied by TGA. Pure sodium chloride was added in the ionic liquid solution ([BMImCl] = 30 $mmol.L^{-1}$) until reaching Na^+ concentrations of 0.1 $mol.L^{-1}$, 1 $mol.L^{-1}$ and 4 $mol.L^{-1}$. TGA curves (not shown)

indicated that the amount of ionic liquid intercalated slightly decreased for Na^+ concentrations at least equal to 1 mol.L^{-1}. However, at 900°C, a difference of less than 4 mass. % was measured between the weight losses of the intercalated clays prepared with 4 mol.L^{-1} NaCl and without NaCl. These results suggest a strong affinity of montmorillonite for the organic $BMIm^+$ cation, and probably also for the other organic cations studied.

3.1.3 FTIR analyses

The infrared spectra of pure montmorillonite and RTILs-intercalated montmorillonites exhibited similar bands in the region 400-1300 cm^{-1} (Figure 5) related to the structure of montmorillonite. The swelling of the clay by intercalation of the RTILs did not affect the frequencies of the structural adsorption bands. The large band observed at 1040 cm^{-1} on all the spectra, with three shoulders at 1090 cm^{-1}, 1120 cm^{-1} and 1175 cm^{-1} were attributed to the Si-O stretching vibration of montmorillonite [34]. The low intensity peaks observed at 938 cm^{-1}, 911 cm^{-1} and 864 cm^{-1} were assigned to the OH bending mode of the Al_2OH, Fe(III)AlOH and MgAlOH groups, respectively [35]. The band at 634 cm^{-1} was assigned to the stretching vibration of the Al-O bonds whereas both bands observed at 530 cm^{-1} and 471 cm^{-1} were attributed to the Mg-O bonds [18]. The vibration bands of water gave two signals (Figure 6) : a broad band at 3460 cm^{-1} attributed to the OH asymmetric and symmetrical stretching vibrations (ν-OH), and a peak at 1660 cm^{-1} assigned to the bending vibrations (δ-OH). The peak at 3645 cm^{-1} was attributed to the hydroxyl groups of the montmorillonite layer [36].

Infrared spectra of intercalated montmorillonites (Figures 5b to 5f and 6b to 6f) indicated the occurrence of the organic functionalities of the different ionic liquids. The small peaks in the region 1400-1500 cm^{-1} were characteristic of the asymmetric bending vibrations of the CH_2 and CH_3 groups of the alkyl chains (Figures 6b to 6f). The new signal appearing at 1593 cm^{-1} on the spectra of the three imidazolium intercalated MMTs (Figure 6b to 6d) was the signature of the stretching of $(N)CH_2$ and $(N)CH_3CH$ bonds of the cycle. No signal was observed in the same position on the spectra of the pyridinium intercalated MMTs (Figures 6e and 6f). However, for these two materials, the band observed at 1660 cm^{-1} was broadened suggesting the presence of a small amount of water.

The $\nu_{as}(CH_2)$ and $\nu_s(CH_2)$ signals, characteristic of the hydrocarbon chain are observed with a varying intensity in the 2850-3000 cm^{-1} region. A very weak signal near to ~ 3190 cm^{-1} observed on the spectra of the imidazolium intercalated compounds (Figure 6b to 6d) can be attributed to the ν(N-H) band.

On spectrum of the $AMIm^+$ intercalated montmorillonite (Figure 6d), the peak around 1600 cm^{-1} can be attributed to the stretching of the C=C alkenes functional group.

The presence of the characteristic bands of the different ionic liquids on the infrared spectra of the organic-loaded montmorillonites highlights the efficiency of the adsorption process.

3.2 Adsorption isotherms of ionic liquids

3.2.1 Adsorption isotherms at 25°C

The presence of the alkyl chains confers an hydrophobic character to the used ionic liquids. For this reason, the dissolved ionic liquid cations showed a great affinity for montmorillonite and thus were exchanged with the interlayer mineral cations (mainly Na^+). Kinetic studies (not shown) displayed that for the five ionic liquids, the adsorption kinetic was very quick. After only 1 minute of contact time, whatever the ionic liquid cation, more than 80 % of cation was exchanged. The maximum adsorption equilibrium was reached at least after 15 minutes of contact with the adsorbent. Kinetics were better reproduced by the pseudo-second order model ($R^2 > 0.99$) than the pseudo-first order one ($R^2 > 0.98$). At 25°C, high adsorption amounts were observed on the isotherms at the lowest adsorbate concentrations ($Ce < 0.5$ $mmol.L^{-1}$) indicating the strong RTILs interactions with the surface of the clay layers occurring at low concentration. All the isotherms reached a plateau at high concentrations indicating the presence of strong adsorption sites. The adsorption capacities of the various RTILs on MMT were found to depend on their size and on the chemical nature of the cation. The adsorption uptake increased as the length of the alkyl chain of the imidazolium or pyridinium cation decreased (Figure 7). For a same alkyl substituent, the affinity was the highest for the pyridinium salts compared to the imidazolium ones probably because pyridinium salts are more hydrophobic than imidazolium ones. The highest adsorption capacity was obtained for BPyBr (Figure 7 : ~ 96 mmol/100g) and the lowest one for OMImCl (Figure 7 : ~ 72 mmol/100g). These observations were in agreement with the TGA results, suggesting that the affinity of the clay towards the different RTILs followed the order : BPyBr > OPyBr ~ AMImCl ~ BMImCl > OMImCl. The adsorption capacity values were lower than the cation exchange capacity pointing out that the cationic exchange was incomplete . For a CEC equal to 115 mmol/100 g, the theoretical number of exchangeable ion would be of ~ 7.10^{20} ions per gram of material. By assuming that the internal surface of a MMT is about 400 $m^2.g^{-1}$ [37] for a complete cationic exchange, the maximum theoretical surface available for an interlayer compensation cation would be of $400/7.10^{20}$ ~ $55.8\ 10^{-20}$ m^2. This means that if the average size of an alkyl ion lying flat in the interlamellar space is higher than ~ 56 $Å^2$, the exchange with the mineral cations can not be complete. These steric considerations could explain the fact that the adsorption capacity of MMT was higher for the butyl and allyl ionic liquids (from which calculated surface ~ 35-45 $Å^2$, Table 1) than for the octyl ones (from which calculated surface ~ 65-70 $Å^2$, Table 1). The higher adsorption on

MMT for pyridinium salts than for imidazolium analogous might be due to the difference in their hydrophobic character that might be more pronounced for pyridinium cations [24, 38]. Analyses of the sodium concentrations in the different solutions after the intercalations were in agreement with the amounts of RTILs inserted in the interfoliar space, justifying the cationic exchange mechanism.

3.2.2 Adsorption isotherm at different temperatures, thermodynamic study

Adsorption isotherms at 40°C and 55°C exhibited similar profiles as those studied at 25°C (Figures 8, 9 and 10).The affinity of MMT for the 5 RTILs followed the same order for the three investigated temperatures. The adsorption capacity of the different RTILs onto MMT increased as the temperature increased from 25°C to 55°C.
Langmuir and Freundlich models did not give satisfying results to fit the experimental data (at 25°C, for the Freundlich model, R^2 was in the range 0.78 - 0.87, whereas for the Langmuir model, R^2 was in the range 0.87 - 0.97). The IL uptake was governed mainly by the ionic exchange instead of an adsorption on the basal surface. The profile of the isotherms was typical of ionic exchange as they were possibly fitted using the relation :$Ce= a\times qe^2/ (b-qe)$, resulting from the previous equation of K_{ex}, in which a and b are constant parameters depending on experimental conditions (at 25°C, $0.94 < R^2 < 0.97$).

In order to obtain the thermodynamic parameters, the isotherms Ce = f(qe) at 25°C, 40°C and 55°C were fitted using spline functions (polynomials of degree 5). The isosteric Gibbs free energy ΔG° of adsorption of the different ionic liquids onto MMT was calculated from the law of mass action using the equilibrium constant of exchange ($K_{ex}=([Na^+]_{solution}\times[RTIL^+]_{clay})/([Na^+]_{clay}\times[RTIL^+]_{solution})$) determined as follows, assuming the electrical neutrality and an homoionic Na-MMT: $K_{ex} = (qe\times qe\times m_{MMT}/100/V)/(Ce\times(CEC - qe))$, where Ce is the organic cation concentration in the solution at equilibrium ($mmol.L^{-1}$), qe is the amount of intercalated cation ($RTIL^+$) for 100g of MMT (mmol/100g), CEC is the cation exchange capacity of the Na-montmorillonite used (115 mmol/100g), V is the total solution volume (L) and m_{MMT} is the mass of adsorbent (g) used for the isotherms studies.

Average ΔG° values were calculated from qe values in the range 32-64 mmol/100g (Table 3). The average isosteric enthalpy ΔH° and entropy ΔS° of adsorption were also calculated from the slope and the intercept of the plot of $Ln(K_{ex})$ versus 1/T using the equation : $\Delta G° = \Delta H° - T\Delta S°$. Thermodynamic parameters were computed for the adsorption of the five ionic liquids (Table 3).
The positive values obtained for ΔH° (Table 3) were consistent with the increase of the adsorption capacities as the temperature increased from 25°C to 55°C (Figures 8, 9 and 10)

and indicated that the adsorption was an endothermic process. ΔG° values were very close for the 5 RTILs indicating similar adsorption mechanisms on similar adsorption sites. The negative ΔG° values obtained indicated that the adsorption was spontaneous, as attempted according to the hydrophobic character of the different ionic liquids. The positive values of ΔS° could indicate an increase of the disorder at the MMT-solution interface probably due to the desorption of water molecules as the ionic liquids were adsorbed in the interlayer space. This could be related to the TGA analyses of the RTIL-intercalated MMT proving the absence of interfoliar water after the RTILs exchange.

4. Conclusion

This work demonstrates that Na-montmorillonite is a potential adsorbent for ionic liquids cations solubilised in liquid wastes. Characterizations by X-ray diffraction, infrared spectroscopy and thermogravimetric analyses confirmed the intercalation of the alkyl imidazolium and pyridinium cations in the interlayer space of montmorillonite. The mechanism involved is a cationic exchange with the interfoliar Na^+ ions, as confirmed by flame spectroscopy analyses of the recovered solutions after adsorption. Results showed that the affinity between montmorillonite and the different ionic liquids was dependent on the nature of the organic cation and on the length of the grafted alkyl chain. The steric hindrance and the hydrophobicity of the ionic liquid molecules have an influence on the adsorption process.

Adsorption isotherms, studied at pH = 7 and at 25°C, displayed that the maximum adsorption capacity of the substrates followed the order BPyBr > OPyBr ~ AMImCl ~ BMImCl > OMImCl. The maximum adsorption capacity of the used montmorillonite at 25°C is ~96 mmol/100g in the case of BPyBr. Adsorption capacities increased as temperature increased for the five studied ionic liquids. Even if the adsorption capacity of the clay is a little lower than the capacities determined for activated carbons (i.e. ~ 1.4 $mmol.g^{-1}$ for the adsorption of $OMImPF_6$ [6]), phyllosilicates of the smectite group such as montmorillonite constitute interesting adsorbents as their regeneration from the polluted solutions is very easy.

Table captions

Table 1 : developed formula and average sizes of the imidazolium and pyridinium ionic liquid cations

Name	Formula	Size[a] (L x w x h) Å^3
$BMIm^+$	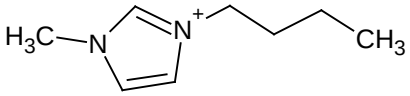	9.97 x 4.30 x 1.82
$OMIm^+$	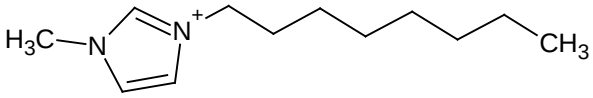	14.90 x 4.28 x 1.81
$AMIm^+$	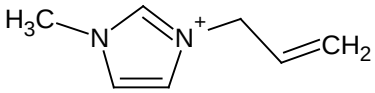	8.63 x 4.30 x 1.82
BPy^+	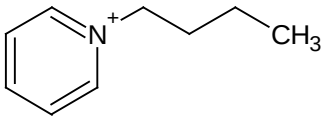	9.59 x 4.99 x 1.82
OPy^+	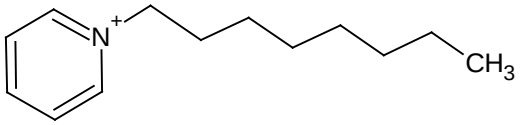	14.44 x 5.00 x 1.81

[a]calculated with ChemSketch [26] from a linear configuration (L = length, w = width, h = height)

Table 2 : d-spacings of the raw and RTILs-intercalated MMTs calculated from XRD patterns

	Raw MMT	AMImCl	BMImCl	OMImCl	BPyBr	OPyBr
d-spacing (Å)	12.13	12.80	13.69	13.80	13.59	13.91
Change in d-spacing vs MMT (Å)	-	0.67	1.56	1.67	1.46	1.78

Table 3 : average isosteric Gibbs free energy, enthalpy and entropy of adsorption of the different RTILs (for qe in the range 32-64 mmol/100g)

IL type	AMImCl	BMImCl	OMImCl	BPyBr	OPyBr
$\Delta G°$ (298K) kJ.mol^{-1}	-4.4	-3.8	-3.8	-4.7	-4.1
$\Delta S°$ (298K) J.K^{-1}.mol^{-1}	36.7	31.0	34.2	45.0	47.0
$\Delta H°$ (298K) kJ.mol^{-1}	6.5	5.4	6.4	8.7	9.9

Figure captions

L. Reinert et al. Figure 1

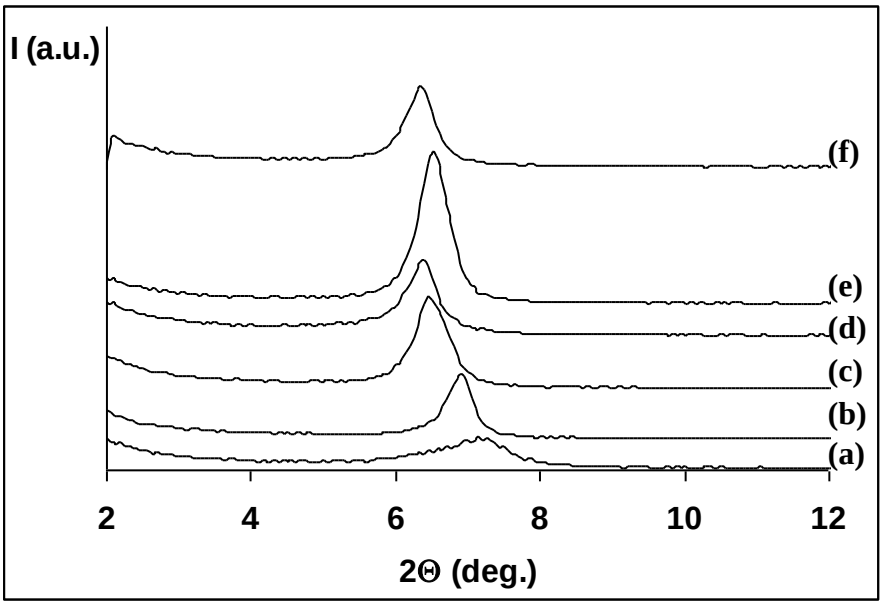

Figure 1 : X-ray diffraction patterns of montmorillonite samples : raw montmorillonite (a) and after adsorption of AMImCl (b), BMImCl (c), OMImCl (d), BPyBr (e) and OPyBr (f)

L. Reinert et al. Figure 2

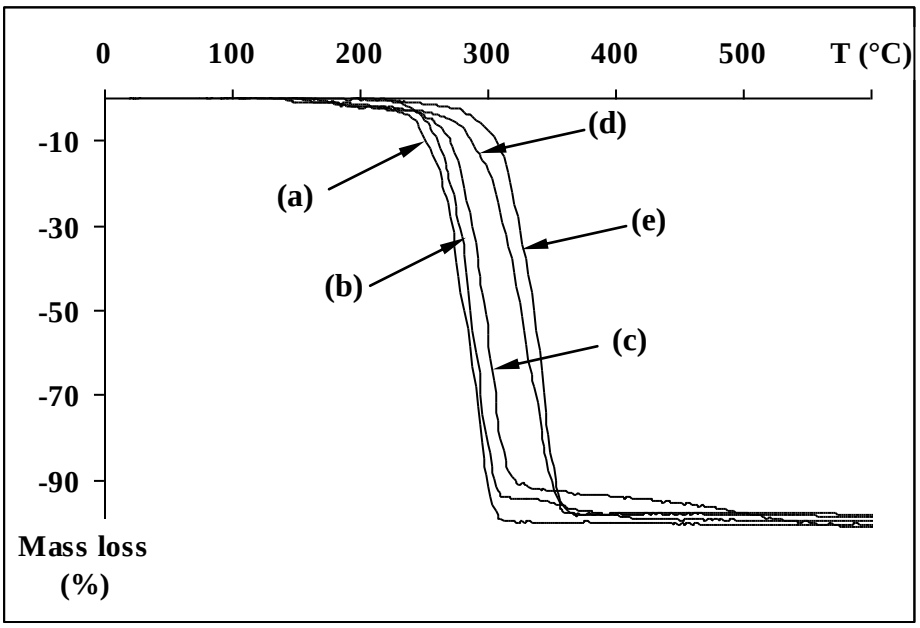

Figure 2 : TGA curves of pure OPyBr (a), BPyBr (b), AMImCl (c), OMImCl (d) and BMImCl (e)

L. Reinert et al. Figure 3

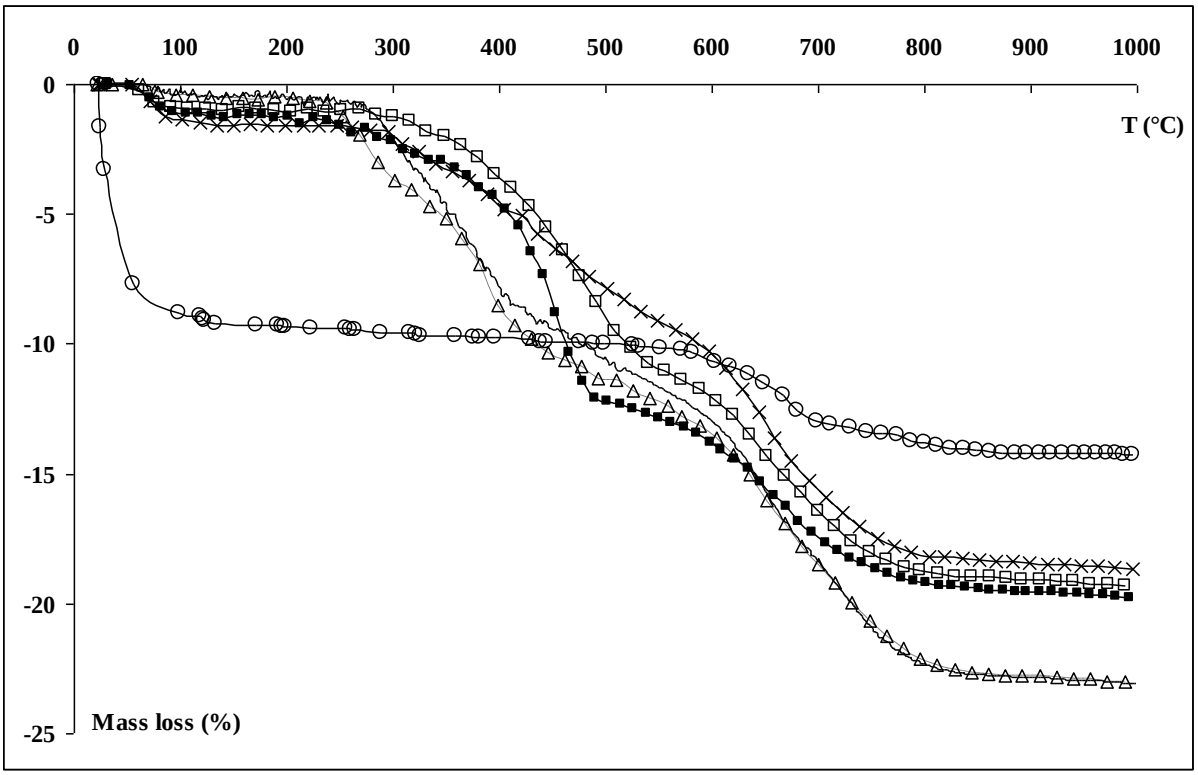

Figure 3 : TGA curves of montmorillonite samples : raw (O) and after adsorption of BMImCl (□), OMImCl (no symbol, full line), OPyBr (Δ), BPyBr (■) and AMImCl (×).

L. Reinert et al. Figure 4

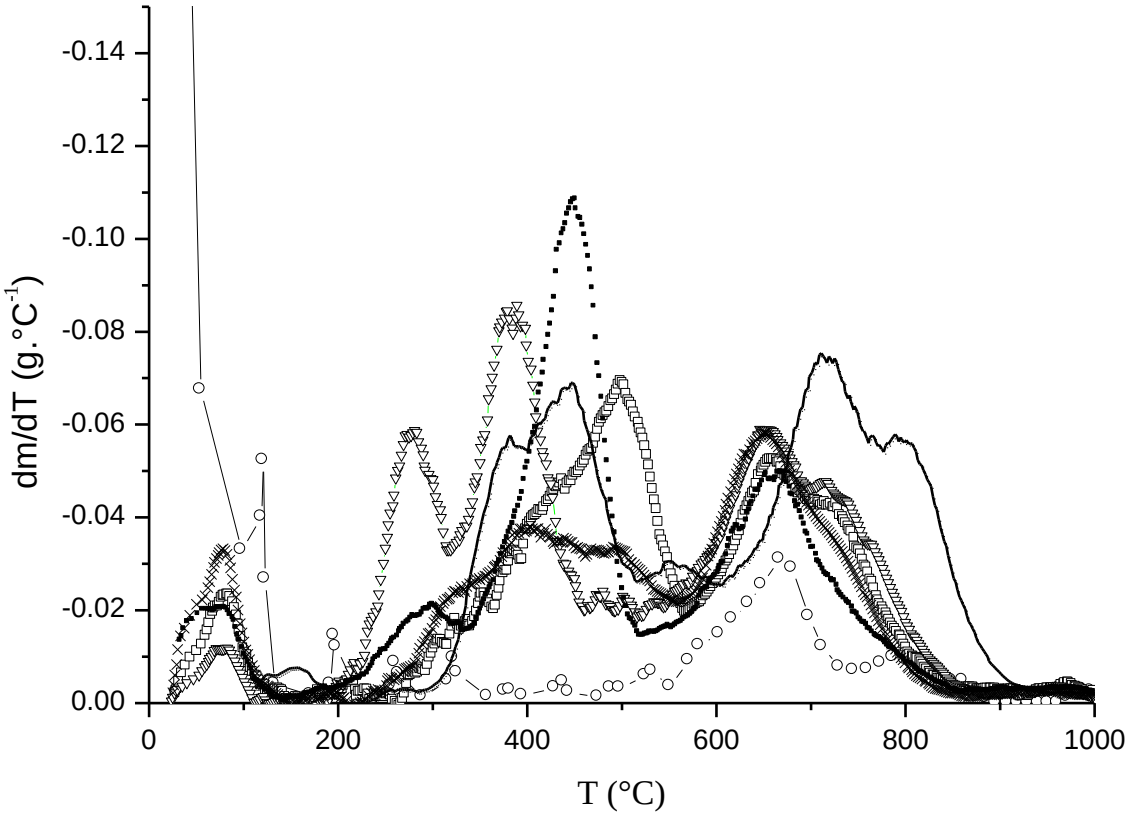

Figure 4 : DTG curves of montmorillonite samples : raw (O) and after adsorption of BMImCl (□), OMImCl (no symbol, full line), OPyBr (Δ), BPyBr (■) and AMImCl (×).

L. Reinert et al. Figure 5

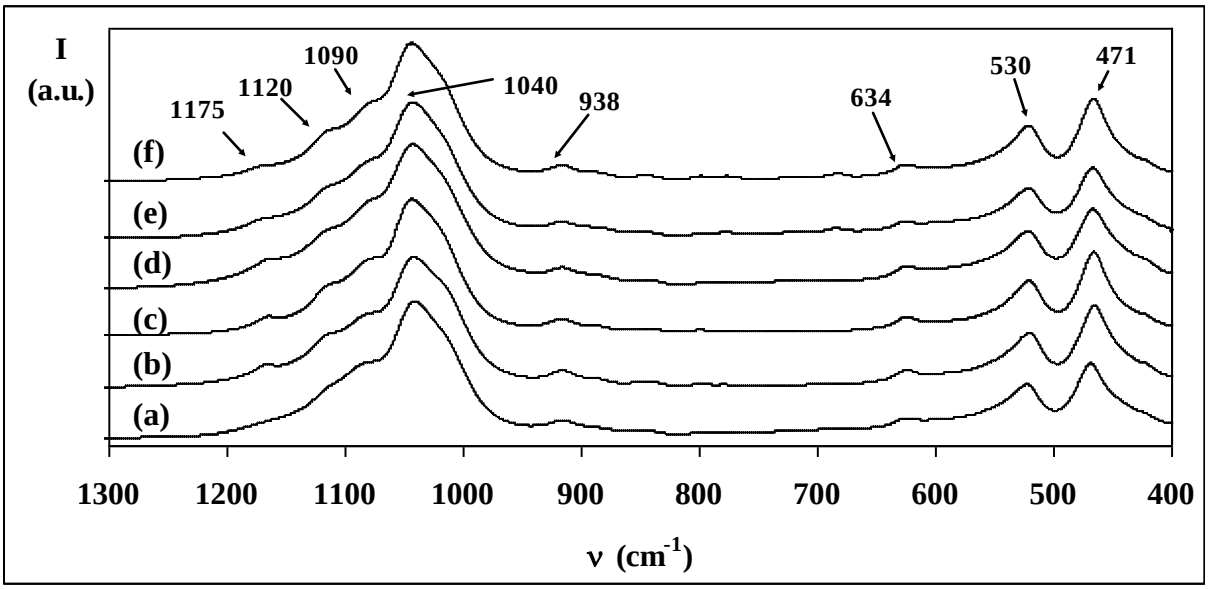

Figure 5 : FTIR spectra in the range 400-1300 cm^{-1} of montmorillonite samples: raw (a), and after adsorption of BMImCl (b), OMImCl (c), AMImCl (d), BPyBr (e) and OPyBr (f).

L. Reinert et al. Figure 6

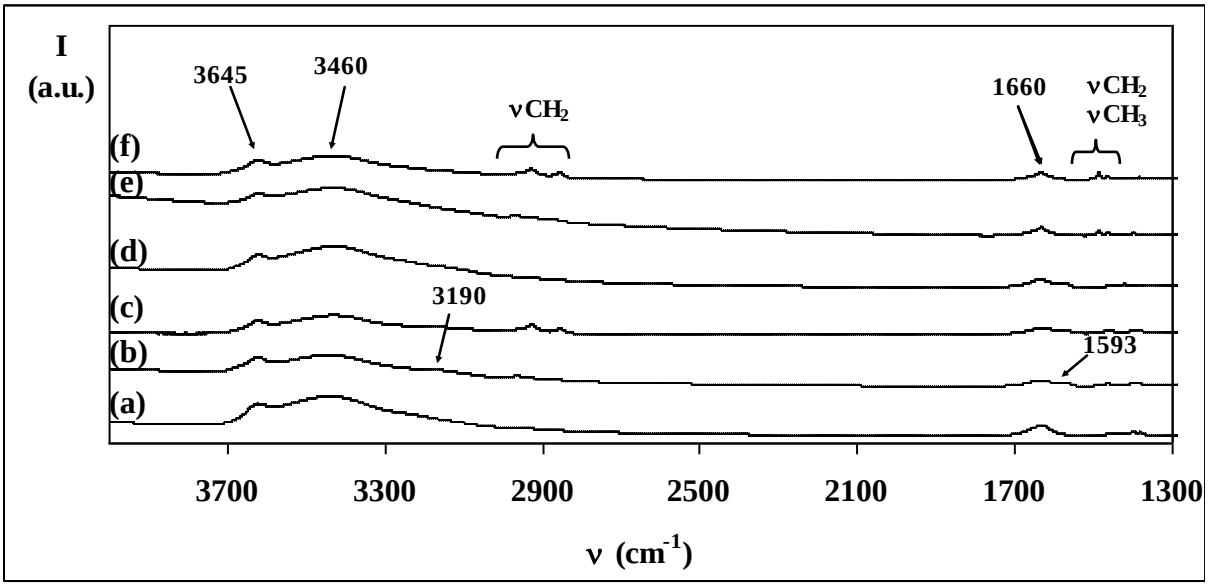

Figure 6 : FTIR spectra in the range 1300-4000 cm^{-1} of montmorillonite samples: raw (a), and after adsorption of BMImCl (b), OMImCl (c), AMImCl (d), BPyBr (e) and OPyBr (f).

L. Reinert et al. Figure 7

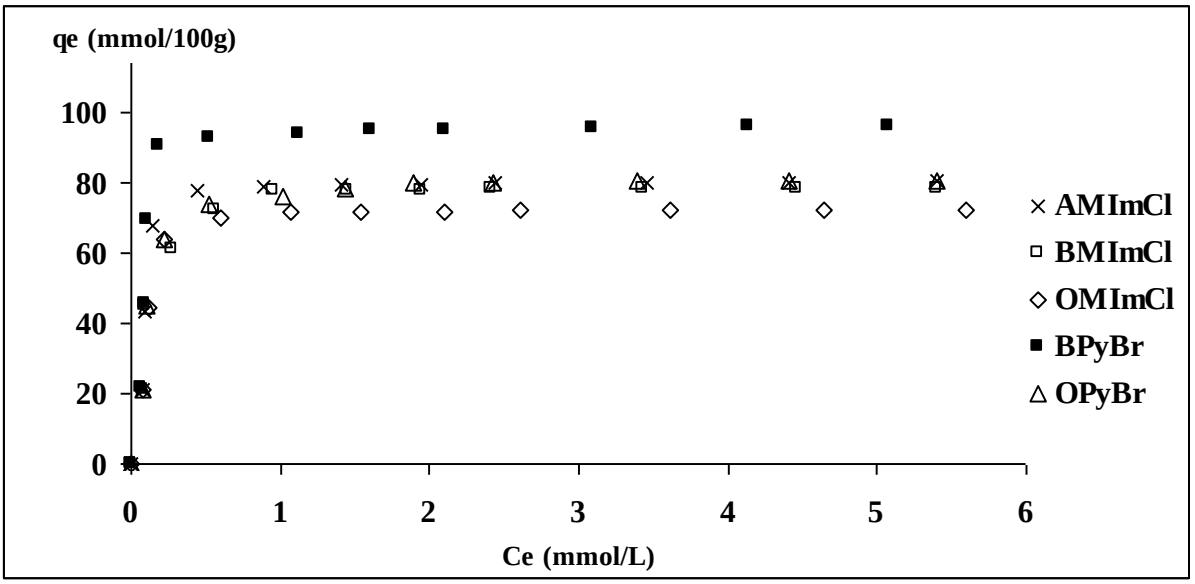

Figure 7 : adsorption isotherms of the five ionic liquids onto MMT at 25°C ([RTILs] = 0-7 $mmol.L^{-1}$, $m_{adsorbent}$ = 0.05 g, V_{LI} = 25 mL, contact time = 24 h)

L. Reinert et al. Figure 8

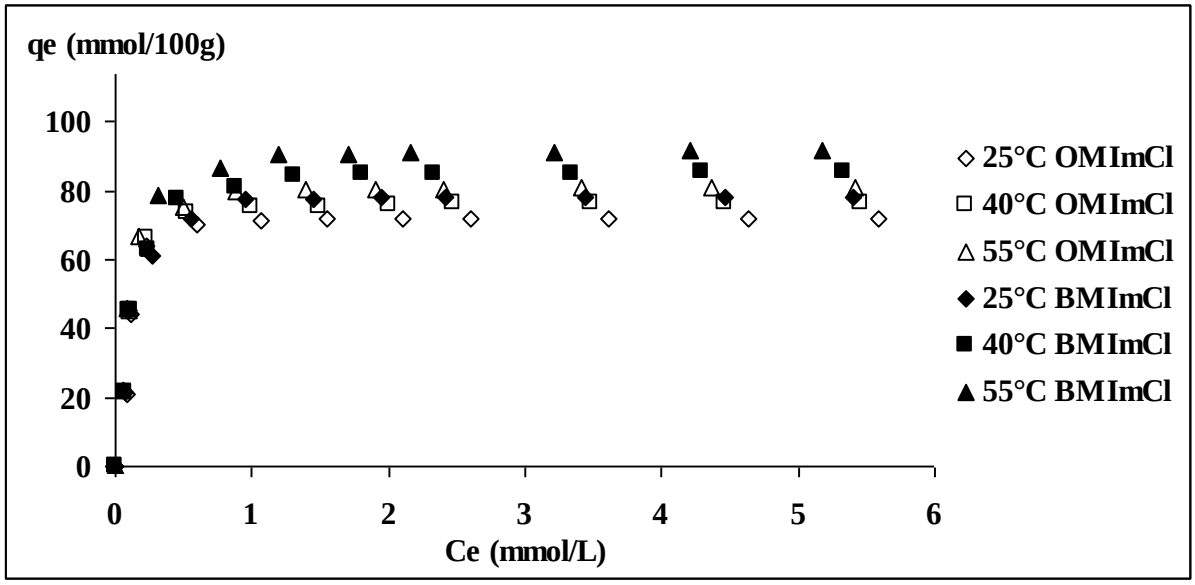

Figure 8 : experimental adsorption isotherms of OMImCl and BMImCl at 25°C, 40°C and 55°C.

L. Reinert et al. Figure 9

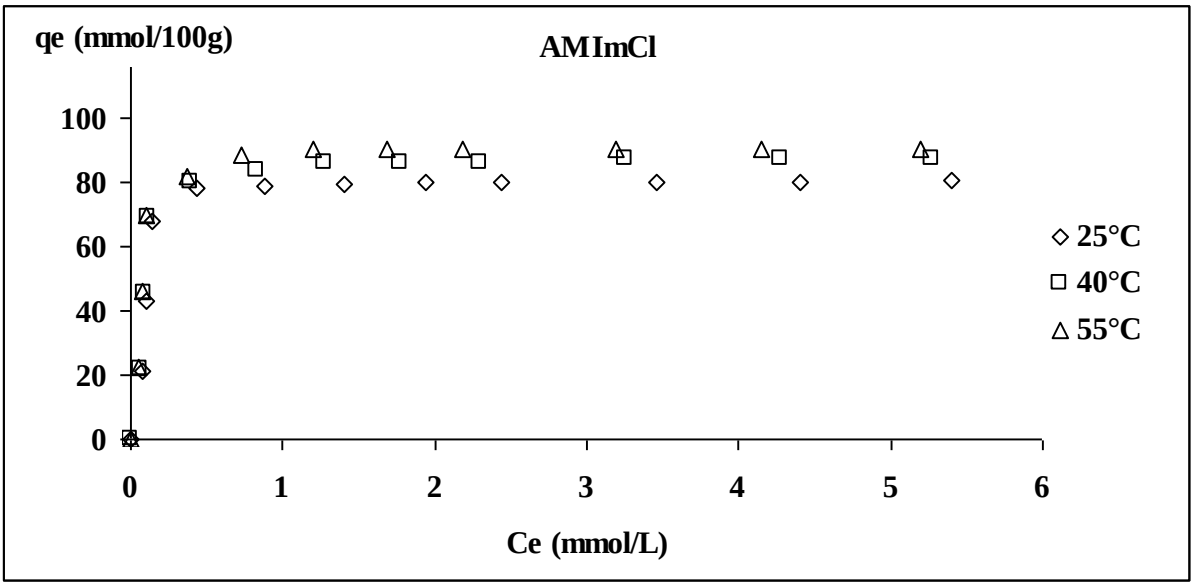

Figure 9 : experimental adsorption isotherms of AMImCl at 25°C, 40°C and 55°C.

L. Reinert et al. Figure 10

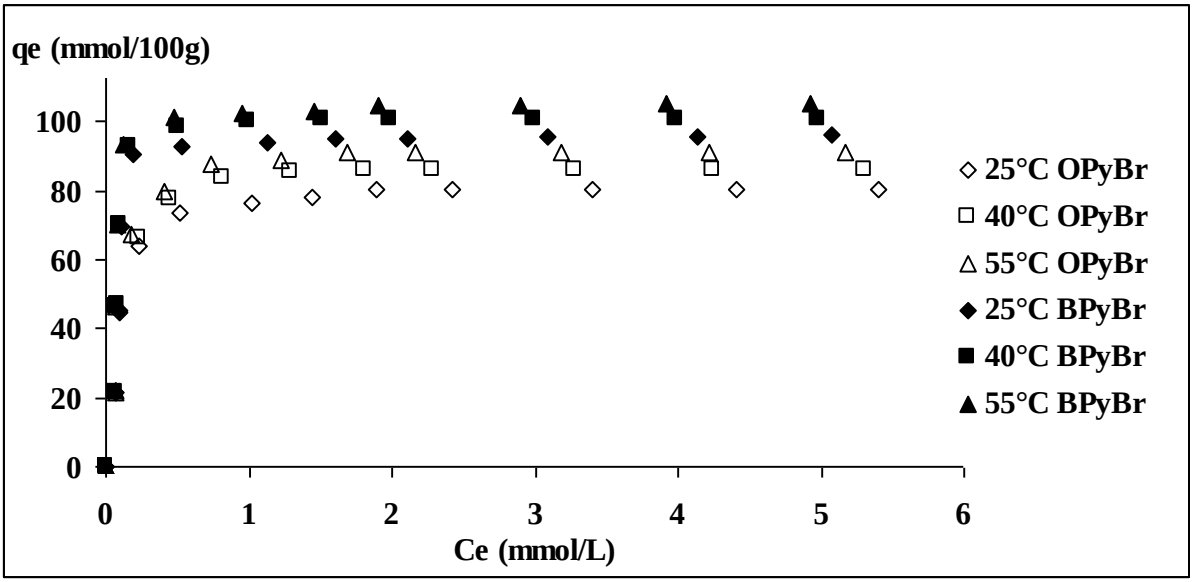

Figure 10 : experimental adsorption isotherms of BPyBr (full symbols) and OPyBr (empty symbols) at 25°C, 40°C and 55°C.

References

[1] R. Wasserscheid, T. Welton, Ionic Liquids in Synthesis, second ed., Wiley-VCH, 2008.

[2] B. Jastorff, R. Störmann, J. Ranke, K. Mölter, F. Stock, B. Oberheitmann, W. Hoffmann, J. Hoffmann, M. Nüchter, B. Ondruschka, J. Filser, How sustainable are ionic liquids? Structure–activity relationships and biological testing as important elements for sustainability evaluation, Green Chem. 5 (2003) 136-142.

[3] R.D. Rogers, K.R. Seddon, S. Volkov, Green Industrial applications of Ionic Liquids, 1st ed., Springer, 2003.

[4] V.K. Ahluwalia, R.S. Varma, Green Solvents for Organic Synthesis, 1st ed., Alpha Science International Ltd., 2009.

[5] T.P. Thuy Pham, C.-W. Cho, Y.-S. Yun, Environmental fate and toxicity of ionic liquids: A review, Water Res. 44 (2010) 352-372.

[6] J. Palomar, J. Lemus, M.A. Gilarranz, J.J. Rodriguez, Adsorption of ionic liquids from aqueous effluents by activated carbon, Carbon 47 (2009) 1846-1856.

[7] H.Y. Wang, D.X. Han, A new method of immobilizing ionic liquids into layered zirconium phosphates, Chinese Chem. Lett. 18 (2007) 764-767.

[8] M.E. Mahmoud, H.M. Al-Bishri, Supported hydrophobic ionic liquid on nano-silica for adsorption of lead, Chem. Eng. J. 166 (2011) 157-167.

[9] M. Matzke, K. Thiele, A. Müller, J. Filser, Sorption and desorption of imidazolium based ionic liquids in different soil types, Chemosphere 74 (2009) 568-574.

[10] P. Stepnowski, Preliminary assessment of the sorption of some alkyl imidazolium cations as used in ionic liquids to soils and sediments, Aust. J. Chem. 58 (2005) 170-173.

[11] J.J. Beaulieu, J.L. Tank, M. Kopacz, Sorption of imidazolium-based ionic liquids to aquatic sediments, Chemosphere 70 (2008) 1320-1328.

[12] S. Letaief, T.A. Elbokl, Ch. Detellier, Reactivity of ionic liquids with kaolinite: Melt intercalation of ethyl pyridinium chloride in an urea-kaolinite pre-intercalate, J. Colloid Interface Sci. 302 (2006) 254-258.

[13] S. Letaief, Ch. Detellier, Ionic liquids-kaolinite nanostructured materials. Intercalation of pyrrolidinium salts, Clays and Clay Miner. 56 (2008) 82-89.

[14] R. Srivastava, S. Fujita, M. Arai, Synthesis and adsorption properties of smectite-like materials prepared using ionic liquids, Appl. Clay Sci. 43 (2009) 1-8.

[15] J.W. Gilman, W.H. Awad, R.D. Davis, J. Shields, R.H. Harris Jr., C. Davis, A.B. Morgan, T.E. Sutto, J. Callahan, P.C. Trulove, H.C. DeLong, Polymer/Layered Silicate Nanocomposites from Thermally Stable Trialkylimidazolium-Treated Montmorillonite, Chem. Mater. 14 (2002) 3776-3785.

[16] F.A. Bottino, E. Fabbri, I.L. Fragalà, G. Malandrino, A. Orestano, F. Pilati, Polystyrene-Clay nanocomposites prepared with polymerizable imidazolium surfactants, Macromol. Rapid Commun. 24 (2003) 1079-1084.
[17] A.B. Morgan, J.D. Harris, Exfoliated polystyrene-clay nanocomposites synthesized by solvent blending with sonication, Polymer 45 (2004) 8695-8703.
[18] N.H. Kim, S.V. Malhotra, M. Xanthos, Modification of cationic nanoclays with ionic liquids, Microporous and Mesoporous Mater. 96 (2006) 29-35.
[19] G. Chigwada, D. Wang, C.A. Wilkie, Polystyrene nanocomposites based on quinolinium and pyridinium surfactants, Polym. Degrad. Stab. 91 (2006) 848-855.
[20] D.J. Greenland, J.P. Quirk, Adsorption on 1-n-alkylpyridinium bromides by montmorillonites, Proceedings of the Ninth National Conference on Clays and Clay Minerals, Swinefort A. ed., Pergamon Press, New York, 1962, pp. 484-499.
[21]G. Lagaly, M. Ogawa, I. Dékány, Handbook of Clay Science, F. Bergaya, B.K.G. Theng, G. Lagaly (eds.), Elsevier, Amsterdam, 2006.
[22] M. Deetlefs, K.R. Seddon, Improved preparations of ionic liquids using microwave irradiation, Green Chem. 5 (2003) 181-186.
[23] H. Zhang, J. Wu, J. Zhang, J. He, 1-Allyl-3-methylimidazolium Chloride Room Temperature Ionic Liquid: A New and Powerful Nonderivatizing Solvent for Cellulose, Macromolecules 38 (2005) 8272-8277.
[24] N. Papaiconomou, N. Yakelis, J. Salminen, R. Bergman, J.M. Prausnitz, Synthesis and Properties of Seven Ionic Liquids Containing 1-Methyl-3-octylimidazolium or 1-Butyl-4-methylpyridinium Cations, J. Chem. Eng. Data 51 (2006) 1389-1393.
[25] K.M. Docherty, C.F. Kulpa Jr., Toxicity and antimicrobial activity of imidazolium and pyridinium ionic liquids, Green Chem. 7 (2005) 185-189.
[26] J.G. Huddleston, D. Willauer, R.P. Swatloski, A.E. Visser, R.D. Rogers, Room temperature ionic liquids as novel media for 'clean' liquid–liquid extraction, Chem. Commun. 16 (1998) 1765-1766.
[27] ChemSketch ACD/Labs 12.0, Advanced Chemistry Development, Inc. 8 King Street East, Suite 107, Toronto, Ontario, Canada M5C 1B5.
[28] C.P. Fredlake, J.M. Crosthwaite, D.G. Hert, S.N.V.K. Aki, J.F. Brennecke, Thermophysical Properties of Imidazolium-Based Ionic Liquids, J. Chem. Eng. Data, 49 (2004) 954-964.
[29] J.M. Crosthwaite, M.J. Muldoon, J.K. Dixon, J.L. Anderson, J.F. Brennecke, Phase transition and decomposition temperatures, heat capacities and viscosities of pyridinium ionic liquids, J. Chem. Thermodyn. 37 (2005) 559-568.
[30] Y. Hao, J. Peng, S. Hu, J. Li, M. Zhai, Thermal decomposition of allyl-imidazolium-based ionic liquid studied by TGA–MS analysis and DFT calculations, Thermochim. Acta 501 (2010) 78-83.

[31] W.H. Awad, J.W. Gilman, M. Nydena, R.H. Harris Jr., T.E. Sutto, J. Callahan, P.C. Trulove, H.C. DeLong, D.M. Fox, Thermal degradation studies of alkyl-imidazolium salts and their application in nanocomposites, Thermochim. Acta 409 (2004) 3-11.
[32] K. Emmerich, F.T. Madsen, G. Kahr, Dehydroxylation behavior of heat-treated and steam-treated homoionic cis-vacant montmorillonites, Clays and Clay Miner. 47 (1999) 91-604.
[33] S.K. Goswami, S. Ghosh, L.J. Mathias, Thermally stable organically modified layered silicates based on alkyl imidazolium salts, J. Colloid Interface Sci. 368 (2012) 366-371.
[34] L. Lerot, P.F. Low, Effect of swelling on the infrared absorption spectrum of montmorillonite, Clays Clay Miner. 24 (1976) 191-199.
[35] G. Sposito, R. Prost, J.P. Gaultier, Infrared spectroscopic study of adsorbed water on reduced-charge Na/Li-montmorillonites, Clays Clay Miner. 31 (1983) 9-16.
[36] V.C. Farmer, The infrared spectra of minerals, Mineralogical Society, London, 1974.
[37] H. Van Damme, M. Crespin, M.I. Cruz, J.J. Fripiat, Adsorption of safranine by Na^{+}, Ni^{2+} and Fe^{3+} montmorillonites, Clays Clay Miner. 25 (1977) 19-25.
[38] A. Chapeaux, L.D. Simoni, M.A. Stadtherr, J.F. Brennecke, Liquid phase behavior of ionic liquids with water and 1-octanol and modeling of 1-octanol/water partition coefficient. J. Chem. Eng Data 52 (2007) 2462-2467.